Available online at www.sciencedirect.com
SCIENCE DIRECT®
Optics Communications 247 (2005) 133–139
OPTICS COMMUNICATIONS
www.elsevier.com/locate/optcom

Improving the accuracy of homodyne Michelson interferometers using polarisation state measurement techniques

Suat Topcu [a,*], Luc Chassagne [a], Yasser Alayli [a], Patrick Juncar [b]

[a] Department of Physics, LIRIS/CNRS – University of Versailles, 45 Avenue des Etats Unis, 78035 Versailles, France
[b] BNM-INM/CNAM, 75141 Paris, France

Received 12 October 2004; received in revised form 8 November 2004; accepted 9 November 2004

Abstract

We demonstrate a simple homodyne Michelson interferometer design capable of fringe interpolation accuracy of one part in 36,000 leading to a potential accuracy of 10 pm. This improvement becomes possible thanks to the significant advances in polarimetry that permit measurement of the ellipsometric parameters ψ and Δ with an accuracy of 0.01° with readily available commercial equipment. The proposed method has been set up and we make a direct comparison with a commercial heterodyne interferometer by measuring the displacement of the same target mirror. This latter has been displaced by steps of 20 nm using a high accuracy position control method.

PACS: 42.87.Bg; 95.75.Hi; 06.30.−k
Keywords: Single frequency interferometry; Optical nonlinearity; Polarimetry; Metrology

1. Introduction

Photolithography steppers, mask and reticle writers and metrology instruments rely on displacement-measuring interferometers to improve position accuracy. The trends of reducing the minimum feature size, increasing wafer and panel size and increasing throughput pushes the performance requirements for interferometric systems to unprecedented levels. As the field of interferometry tends towards more accurate measurements with ever increasing resolution, heterodyne laser interferometry has replaced homodyne laser interferometry as the basis of metrology and control in numerous high accuracy displacement measurement applications. However homodyne laser interferometry still has some interesting features like its ease of use, its lower cost and more important its

* Corresponding author. Tel.: +33139253023; fax: +33139253025.
E-mail address: suat.topcu@ens-phys.uvsq.fr (S. Topcu).

0030-4018/$ - see front matter © 2004 Elsevier B.V. All rights reserved.
doi:10.1016/j.optcom.2004.11.040

low level of periodic error. Actually, once the classical errors (stability of the laser source, alignment error, vibration, temperature variation and air turbulence) can be kept small enough, then the practical limitations of interferometry will be given by the noise and the nonlinearity due to optical cross talk. As demonstrated by Wu and Su [1], this type of error is of less importance in single-frequency interferometers. For example for a mixing ratio of 0.1 between the two polarization states, the error in a single-frequency interferometer is about 20 times smaller than in a heterodyne interferometer. Although numerous experimental investigations have been performed to measure or to compensate this error on displacement measurements made with heterodyne interferometers [2–5], all the methods suffer from some drawbacks or are too complicate. This kind of considerations gives a renewed interest to homodyne interferometry providing an improved resolution and accuracy levels.

In this paper we demonstrate that the resolution and the accuracy of the homodyne Michelson interferometer could be considerably improved by measuring the polarization state of the laser field at the output of the interferometer. We show that it is possible to interpolate the optical fringe into one part over 36,000 with readily available commercial polarimeters. Using a laser source at a wavelength of 633 nm, one can reach a potential accuracy of 10 pm. The proposed setup has been assembled. We make a direct comparison with a commercial heterodyne interferometer by measuring the displacement of the same target mirror. The target mirror has been displaced step by step and the corresponding displacement has been measured simultaneously by the two interferometers. Subnanometric accuracy is observed in both cases. The last part of the paper is dedicated to the measurement of the periodic nonlinearity of the commercial heterodyne interferometer using our polarimetric interferometer as a reference.

2. Theoretical approach

The basic setup of an ideal heterodyne Michelson interferometer is shown in Fig. 1. The laser emits two partial beams with Gaussian profiles of different angular frequency (ω_1,ω_2) which ideally are linearly polarized and orthogonal to each other. A beamsplitter splits the laser light into two beams, one for reference and the other for measuring, usually with almost equal intensity. One part of the beam passes through a mixing polarizer leading to a reference interference signal collected by a photodetector (PD1). The other part of the beam passes through a polarizing beamsplitter. The two resulting beams are reflected, respectively, by a fixed and a movable mirror. They cover a different path $\Delta\ell$. Quarter-waveplates are used to rotate to 90° the polarization of the beams. Finally, the recombined beam is collected by a photodetector (PD2) after passing through a mixing polarizer. If the waves are assumed to propagate along the positive direction of the z-axis of an s–p–z orthogonal, right-handed, Cartesian coordinate system (Fig. 1), the electromagnetic field components of the laser beam can be represented as

$$E_L(z,t) = \begin{pmatrix} E_s(z,t) \\ E_p(z,t) \end{pmatrix} = \frac{1}{\sqrt{2}} \begin{pmatrix} B\exp\left[-\mathrm{i}(\omega_2 t + \phi_{0s})\right] \\ A\exp\left[-\mathrm{i}(\omega_1 t + \phi_{0p})\right] \end{pmatrix}, \quad (1)$$

where ϕ_{0s} and ϕ_{0p} represent the initial phases of both oscillations.

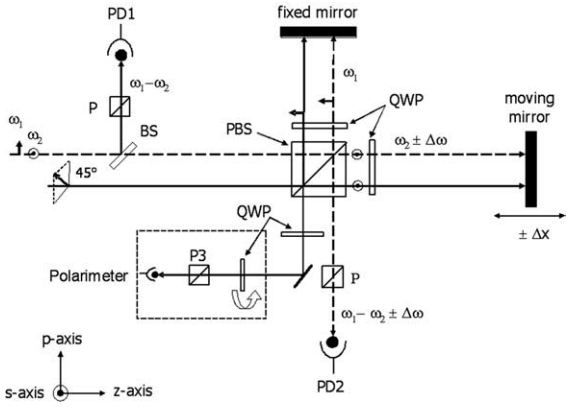

Fig. 1. Schematic representation of the principle of heterodyne (dash line) and homodyne (straight line) laser interferometers: P, polarizer; PBS, polarizing beamsplitter; PD, photodetector; BS, beamsplitter; QWP, quarter-waveplate.

Using the Jones matrices [6–9], the output signal I_{ref} of the beam on photodiode 1 (PD1) is given by

$$I_{\text{ref}} = \tfrac{1}{2}(A^2 + B^2) + AB\cos\left[(\omega_2 - \omega_1)t + (\phi_{0s} - \phi_{0p})\right]. \quad (2)$$

This signal will be used as a reference signal. The same calculation shows that the signal on photodiode 2 (PD2) is equal to

$$I_{\text{meas}} = \tfrac{1}{2}(A^2 + B^2) + AB\cos\left[(\omega_2 - \omega_1)t + (\phi_{0s} - \phi_{0p}) + \Delta\phi\right]. \quad (3)$$

The result is a phase shift of the measurement signal compared to the reference signal given by

$$\Delta\phi = \Delta\omega t = \frac{4\pi n \Delta\ell}{\lambda}, \quad (4)$$

where λ represents the wavelength in vacuum of the laser, $\Delta\omega = \omega_2 - \omega_1$ and n the refractive index of air. Eq. (4) is the well-known formula for a heterodyne interferometer. Commercially available interferometric systems can digitalize at best one interference fringe into 1024 digits achieving a resolution of $\lambda/2048 \simeq 0.31$ nm [10].

Consider now the setup of the homodyne interferometer also represented in Fig. 1. The two main differences compared to the heterodyne one are:

- the laser has only one component oriented at 45° with respect to the p-axis,
- the output of the interferometer is sent into a polarimeter.

Any polarization states can be described with only two parameters (ψ,Δ) as shown in Fig. 2. $\tan(\psi)$ and Δ are, respectively, the amplitude ratio and the phase difference of the p- and s-components of the electromagnetic field. For a linear polarization, the ellipticity Δ is null while it is equal to $\pi/2$ for a right circular polarization state. The most common method to measure ψ and Δ uses a mechanically rotated polarizing element and employs Fourier analysis of the detected signal to calculate ψ and Δ from the amplitudes and the phases of the second and fourth harmonics of the signal. The accuracy on ψ and Δ can reach at best

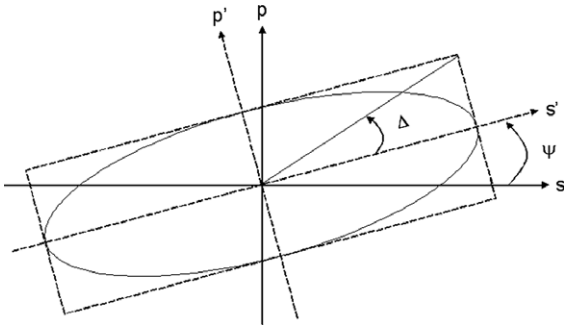

Fig. 2. Definition of the ellipsometric parameters ψ and Δ.

0.001° however most of the inexpansive commercially available polarimeter have an accuracy of 0.01°. A simple mathematical approach of the optical setup is also possible using the Jones matrices calculation. Omitting the temporal and spatial propagation terms, the Jones matrices of the s- and p-components of the laser field at the output of the Michelson interferometer (just after the quarter waveplate placed in front of the polarizing beamsplitter) are:

$$\vec{E}_p = \frac{1}{\sqrt{2}}\begin{pmatrix} 1 \\ -\mathrm{i} \end{pmatrix}, \quad (5)$$

$$\vec{E}_s = \frac{1}{\sqrt{2}}\begin{pmatrix} \exp(\pm\mathrm{i}\phi) \\ \mathrm{i}\exp(\pm\mathrm{i}\phi) \end{pmatrix}, \quad (6)$$

where ϕ is the phase shift induced by the displacement of the mirror. Hence, at the output of the interferometer, we have two circularly polarized components with a phase difference equal to $(\pi/2 \pm \phi)$ according to the sense of the displacement. The total electromagnetic field at the output of the interferometer is

$$\vec{E} = \vec{E}_p + \vec{E}_s = \begin{pmatrix} \cos\phi/2 \\ \mp\sin\phi/2 \end{pmatrix} = \begin{pmatrix} \cos\psi \\ \sin\psi \end{pmatrix}. \quad (7)$$

So the resulting polarization state of the electromagnetic field is then linear and will rotate with an angle ψ about to the p-axis as ϕ varies, i.e., as the mirror moves. Hence, this interferometric setup allows us to link the displacement of the target mirror (via ϕ) to the parameter ψ. As ψ can be measured with an accuracy of 0.01°, it is possible

to interpolate one optical fringe by one part in 36,000 leading to a potential accuracy of $\lambda/72{,}000$ (i.e., $\sim$10 pm for $\lambda = 633$ nm) for a one-pass interferometer. Note that this value is well beyond the fringe interpolation limit of 555,000 due to statistical limits imposed by the laser amplitude noise and detector noise as demonstrated by Meers and Strain [11] and by Lawall and Kessler [12].

3. Experimental

The polarimetric interferometer presented in Fig. 1 has been set up and we make a direct comparison with a commercial heterodyne interferometer (ZMI2001, Zygo) by measuring simultaneously the displacement of the same target mirror. The displacement of the target mirror is controlled using a method more completely described in [13,14] and summarized hereunder.

3.1. Principle of the servo-loop control of the target mirror

The principle of the servo-loop control of the target mirror is sketched in Fig. 3. A function generator puts out two perfect and synchronous sinusoidal signals (s_1, s_2) both at Δv. The two heterodyne components of the laser beam are generated using a Bragg cell fed by a high-stability voltage controlled oscillator (VCO). The signal s_1 is sent to the laser head to phase-lock the VCO while s_2 is sent to a mixer to be phase compared with the signal s_3 coming from the output of the interferometer. If the interferometer is perfect (i.e., without nonlinearities), s_3 is equal to s_1 but with phase-shifts whenever the target mirror moves. If the target mirror is static, both signals s_2 and s_3 are equal in phase and resulting signal ε at the mixer level is null. Suppose that the signal s_2 was phase-shifted by a quantified amount of $2\pi/N$, where N is an integer. If phase-shifts are made periodically with a frequency v_{in} then resulting signal ε is a perfect sinusoidal signal with a frequency equal to v_{in}/N. Finally, if the lock loop containing an actuator supporting the target mirror is closed, the target mirror will move to compensate these phase-shifts thanks to the Doppler effect. In an ideal interferometer, a phase shift of 2π at the output of the interferometer corresponds to a displacement of a target mirror of $\lambda/2$ for a single-pass interferometer. As the phase-shifts on signal s_2 are quantified and equal to $\Delta\phi = 2\pi/N$, the displacement of the target mirror is made step by step with a known step equal to $\Delta p = \lambda/2N$. Note that in practice, due to nonlinearities, ε is not a perfect sinusoidal signal, hence a variation of the optical phase of 2π is not perfectly equal to $\lambda/2$. This point will be discussed hereafter. In our experimental conditions, $\lambda = 633$ nm and $N = 16$. This implies that $\Delta\phi = 0.393$ rad and $\Delta p \approx 20$ nm.

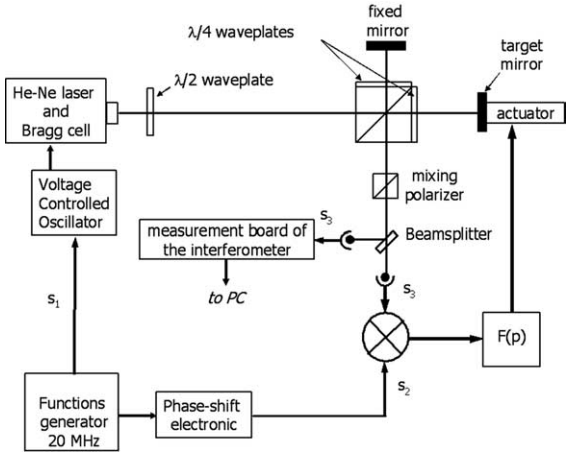

Fig. 3. Principle of the position-control method of the target mirror using a heterodyne laser interferometer.

The heterodyne laser head is a commercial one. The heterodyne components are realized using a Bragg cell and VCO. The beat frequency value between the two laser beam components is equal to 20 MHz. At the output of the Michelson interferometer, the two beams pass through a polarizer that mixes the parallel and overlapping portions of the beams. The processing electronic counts the number of interference fringes and processes it to provide position outputs. The interference fringe is digitized into 1024 digits achieving a resolution of $\lambda/2048 \simeq 0.31$ nm. This corresponds to a phase resolution of 360°/512, or 0.7°, which is 97.7 ps at 20 MHz. The laser head is synchronized to a 20 MHz frequency sinusoidal signal coming from a home-made generator. This

function generator is based on a High Frequency Clock (640 MHz) and a frequency division. The division ratio (obtained with a logic flip-flop components) is 32 in order to have a signal at a frequency of 20 MHz. Phase-shifts on signal s_2 result from the inhibition of one pulse of signal at a frequency of 640 MHz. The inhibitions are pc-controlled with a TTL command signal generated with a direct digital synthesis (DS345, Stanford).

3.2. Experimental setup

There exist several methods for measuring the polarization state of an optical electromagnetic field. In our case, the polarimeter head is composed of a polarizer and a spinning quarter waveplate. Our polarimeter is a commercial one (PA450 Thorlabs). It has a resolution of 0.001° and an accuracy of 0.01°. Both interferometers are mounted under a hermetically sealed box having some windows for the laser beams. The temperature and the pressure inside the box are measured using, respectively, a thermistor PT100 with an accuracy of 5 mK and a pressure sensor (Digiquartz) with an accuracy of 3 Pa. Once the environmental conditions in the box are good enough (i.e., a relative temperature stability of 0.01 °C and a pressure stable at 100 Pa), phase-shifts are sent onto signal s_2 with a frequency of $\nu_{in} = 1$ Hz. Then the displacement of the target mirror is measured simultaneously with both interferometers under the same data acquisition program. The distance between the two beams is less than 10 mm. This distance has been optimized in order to avoid some sources of errors like environmental and mechanical disturbances. The values of ψ and Δ are measured using the polarimeter. We observe that Δ is always equal to 0.00° showing the good quality (short-term) of the polarizing elements, the retardation plates and the coating of the mirrors. The variation of ψ has been converted into displacements. Figs. 4 represents the displacement measured with the two interferometers. Both results are in good agreement even over a displacement range of 1 μm which corresponds to the maximum travel range of the piezoelectric actuator used in our experiment. One can

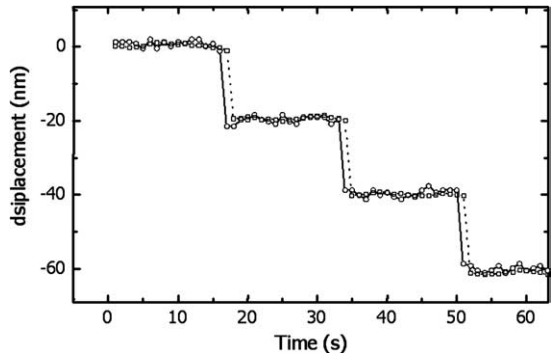

Fig. 4. Optical path changes measured with both interferometers (–○–) homodyne interferometer (–□–) heterodyne interferometer. The target mirror is displaced step by step with a known step of about 20 nm by a piezoelectric actuator.

see that the response given by the polarimeter is slightly delayed compared to the heterodyne interferometer. This is due to the communication port used between the computer and the processing electronics of both systems. The polarimeter uses a RS232 port rather than a PCI-VME card is used for the heterodyne system. PCI-VME cards are known to have a bit rate four orders greater than a RS232 port. Fig. 5 demonstrates that our method is valid whatever the sense of displacement of the target mirror.

The resolution of the interferometer is the minimum detectable displacement of the interferometer target. Practically, we can define the resolu-

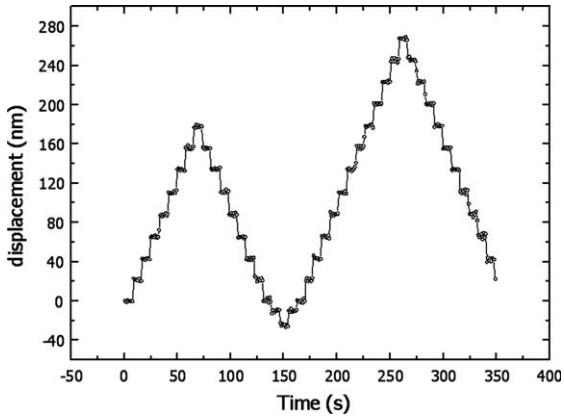

Fig. 5. Nanometric scale representation of the Kefren and Kheops pyramids using our polarimetric interferometer.

tion of a system as the displacement equivalent of one standard deviation of the system noise. The noise level of the two interferometers have been measured simultaneously and under the same environmental conditions. We observe a noise level at 1σ of 313 pm for both interferometers. This noise level is essentially due to the resolution of the heterodyne interferometer equal to 309 pm. Actually as the position of the target mirror is controlled via the heterodyne interferometer we can not expect an uncertainty on the position of the mirror below the resolution of the interferometer. However without this servo loop control, we observe a noise level of several tens of nanometers essentially due to mechanical disturbances. Hence, the resolution of the polarimetric interferometer could be fully improved by making the measurement under vacuum and onto a highly vibration-free table. Another solution is to control the position of the target mirror with the polarimetric interferometer.

4. Application to optical cross talk measurements

In practice, in heterodyne interferometers, the elliptical polarization of the input frequency states, non-orthogonality of the polarizing directions of the incident radiation, misalignment of axis between input polarizing states and the polarizing beamsplitter, and imperfections of the polarizing beamsplitter result in a more complex nonlinear relationship between the measured phase difference and the respective displacement [15]. This periodic error limits the usefulness of heterodyne interferometers from the subnanometre scale for laboratory apparatus to several nanometers for common commercial interferometers. The nonlinearity of the homodyne interferometers arises mainly from the cross talk between the two linearly orthogonal beams of the same frequency and as demonstrated by Wu and Su [1], this type of error is of less importance in homodyne interferometers. Actually, for example for a mixing ration of 0.1 between the two polarization states, the error in a single-frequency interferometer is about 20 times smaller than in the heterodyne interferometer.

Taking into account this result, we decided to measure the periodic error in the heterodyne interferometer using our interferometer as a reference one. In order to minimize the source of nonlinearity due to a misalignment of axis between input polarizing states and the polarizing beamsplitter a half waveplate has been added just after the laser head (Fig. 3) and both axis have been aligned using the frequency spectrum of the electronic signal at the output of the interferometer. We use a spectrum analyzer from ANRITSU (model 2661C). Fig. 6 represents the magnitude of the residual optical beat frequency at the output of the interferometer in one arm of the Michelson interferometer as a function of the azimuthal angle of the half-waveplate. During this measurement the beam travelling through the other arm is stopped. We can see that there exists one angle for which the optical cross talk in both arms can be minimized. The residual nonlinearity is mainly due to the elliptical polarization of the beam components at the output of the laser head and to the separation ratio of the polarizing beamsplitter.

Then the target mirror was displaced over a range equal to $\lambda = 632.991$ nm and the variation of ψ was recorded. Fig. 7(a) and (b) show, respectively, the variation of ψ in a Fresnel representation and as a function of time. Each group of

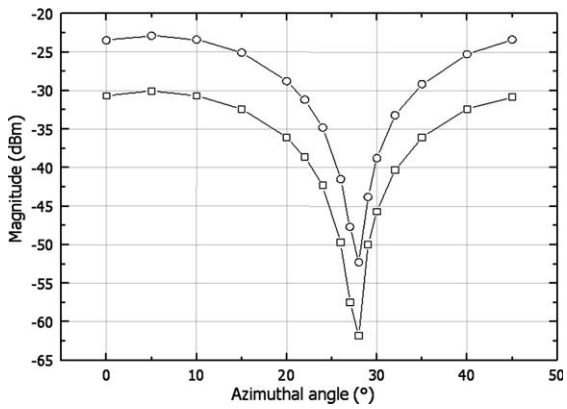

Fig. 6. Frequency spectrum of the signal at the output of the interferometer showing the magnitude of the residual optical beat frequency signal in each arm of the Michelson interferometer as a function of the azimuthal angle of the half-waveplate. Fixed arm (–○–); moving arm (–□–).

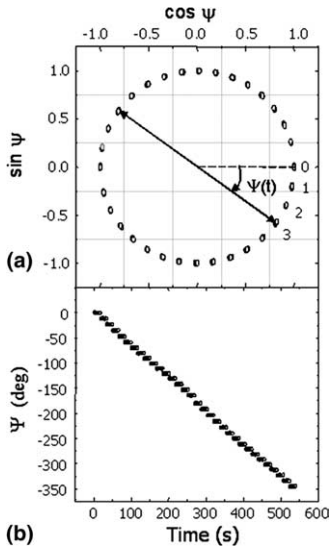

Fig. 7. Variation of ψ as a function of time (b) and in a Fresnel representation (a). Each group of points represents a displacement of the target mirror of $\lambda/32 = 19.781$ nm.

points represents a displacement of the target mirror of $\lambda/32 = 19.781$ nm. We can observe that the slope of the curve represented in Fig. 7(b) is not strictly a straight. This is due to the residual nonlinearity error of the heterodyne interferometer. This effect could be observed in the Fresnel diagram (Fig. 7(a)) by the fact that the angular distance between each group of points is not regular.

To emphasize this point we report in Fig. 8 the angular distance between each point beginning at the point number 0 (Fig. 7(a)). For example between the point 0 and 1, we measure an angular distance of 11.55 instead of 11.25 which corresponds to 360°/32 and so on. The Fig. 8 shows clearly the periodic aspect of this error. The maximum error over one cycle is equal to 2.02° corresponding to an error on the displacement of 3.53 nm. The value given by the manufacturer is about 2 nm.

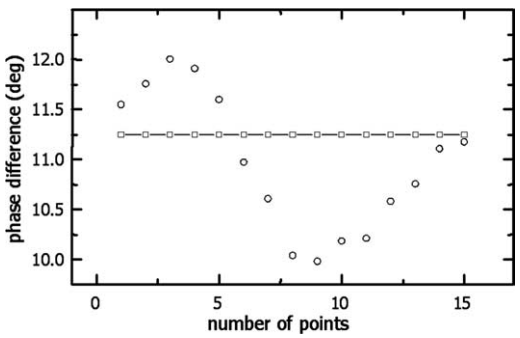

Fig. 8. Angular distance between each point beginning by the point number 0 (Fig. 7(a)). (○) Experimental data; (□) theoretical expected value.

5. Conclusion

We have demonstrated a single frequency interferometer design capable of fringe interpolation with an accuracy of one part in 36,000. The setup has been assembled and validated by making a direct comparison with a commercial heterodyne interferometer. The results show that the accuracy of our apparatus has reached the limit of 310 pm imposed by the resolution of the commercial apparatus which control the position of the target mirror. Finally, our system has been used to measure the periodic nonlinearity error of the heterodyne interferometer. We find a peak-to-peak error up to 3.5 nm with a periodicity of one cycle per fringe in optical path length difference.

References

[1] C. Wu, C. Su, Meas. Sci. Technol. 7 (1996) 62.
[2] W. Hou, G. Wilkening, Prec. Eng. 14 (2) (1992) 91.
[3] C.G.B. Picotto, A. Sacconi, Conf. Proc. Quantum Electron. Plasma Phys. 29 (1991) 361.
[4] A.E. Rosenbluth, N. Bobroff, Prec. Eng. 12 (1) (1990) 7.
[5] S. Patterson, J. Beckwith, in: Eighth IPES Conference, Compiegne, France, 1995, p. 101.
[6] R.C. Jones, J. Opt. Soc. Am. 31 (1941) 488.
[7] R.C. Jones, J. Opt. Soc. Am. 31 (1941) 500.
[8] R.C. Jones, J. Opt. Soc. Am. 32 (1942) 486.
[9] R.M.A. Azzam, N.M. Bashara, Ellipsometry and Polarized Light, Elsevier, Amsterdam, 1989.
[10] F.C. Demarest, Meas. Sci. Technol. 9 (1998) 1024.
[11] B.J. Meers, K.A. Strain, Phys. Rev. A 44 (7) (1991) 44.
[12] J. Lawall, E. Kessler, Rev. Sci. Instr. 71 (7) (2000) 2669.
[13] S. Topcu, L. Chassagne, D. Haddad, Y. Alayli, P. Juncar, Rev. Sci. Instr. 74 (11) (2003) 4876.
[14] S. Topcu, L. Chassagne, D. Haddad, Y. Alayli, P. Juncar, Rev. Sci. Instr. (in press).
[15] S.J.A.G. Cosijns, H. Haitjema, P.H.J. Schellekens, Prec. Eng. 26 (2002) 448.